Analytical Methods

Accepted Manuscript

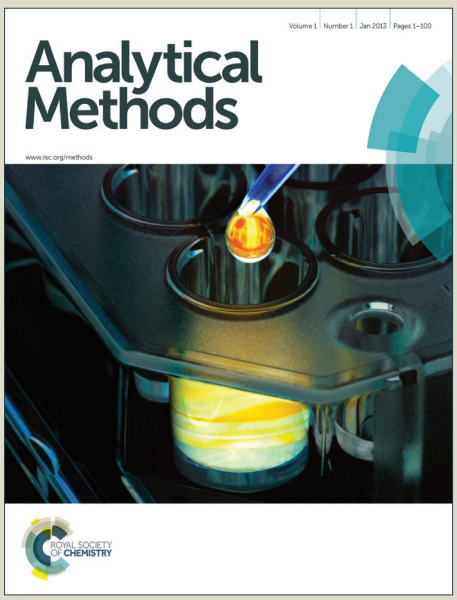

ROYAL SOCIETY OF CHEMISTRY

www.rsc.org/methods

Graphical Abstract:

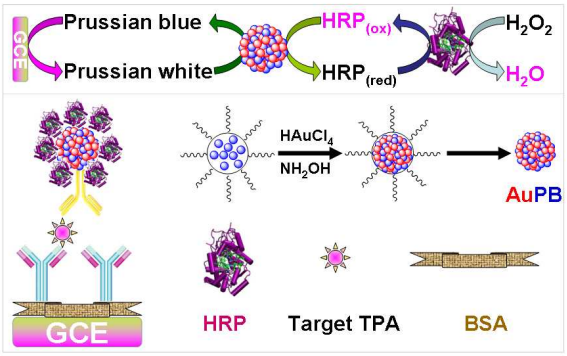

Cite this: DOI: 10.1039/c0xx00000x

www.rsc.org/xxxxxx

ARTICLE TYPE

Biofunctional nanogold microsphere doped with Prussian blue nanoparticles for sensitive electrochemical immunoassay of cancer marker

Qunfang Li,[a,b,*] Fangming Lou,[a] and Dianping Tang[b,*]

Received (in XXX, XXX) Xth XXXXXXXXX 200X, Accepted Xth XXXXXXXXX 200X
DOI: 10.1039/b000000x

A novel signal-amplified strategy for sensitive electrochemical immunoassay of cancer marker (human tissue polypeptide antigen, TPA, used in this case) was developed by using Prussian blue nanoparticles-doped nanogold microsphere (AuPB) as the promoter. To construct such an immunoassay, the AuPB was initially synthesized by using the reverse micelle method, and the as-synthesized AuPB was then heavily functionalized with horseradish peroxidase (HRP) and anti-TPA antibody. Based on a specific sandwich-type immunoassay format, target TPA was monitored on anti-TPA-functionalized glassy carbon electrode by using the biofunctional AuPB as the signal tag. Compared with conventional nanogold labeling, the as-prepared AuPB possessed good redox activity, which could be employed as an electron mediator for improvement of catalytic efficiency of the labeled HRP. Under optimal conditions, the electrochemical immunoassay presented good electrochemical responses toward target TPA, and allowed the detection of TPA at a concentration as low as 5 pg mL^{-1}. The precision, reproducibility, specificity and stablity of the electrochemical immunoassay were acceptable. In addition, the methodology was validated for the analysis of 8 clinic human serum specimens and 8 spiked serum samples, receiving in good accordance with the results obtained from the referenced enzyme-linked immunosorbent assay (ELISA) method.

Introduction

Tissue polypeptide antigen (TPA) is a circulating complex of polypeptide fragments including cytokeratins 8, 18 and 19.[1] It is a differentiation and proliferation marker for non-squamous epithelium and derived neoplasms.[2] Serum levels of TPA have been shown to correlate well with cell growth rate and tumor burden and are elevated in metastatic and disseminated disease.[3] Thus, TPA is valuable as a prognostic marker and for monitoring treatment of patients with different carcinomas.[4] Immunological method, based on the antigen-antibody specific recognition event, has become a major analytical tool for quantitative detection of disease-related proteins.[5] Despite some advances in this field, there is still the request to explore new methods and schemes for improvement of the sensitivity and simplicity of the clinical immunoassays.

Electrochemical immunoassay has attracted increasing interest over the past few years due to the intrinsic advantages, such as good portability, low cost, simple instrumentation, and high sensitivity.[6,7] For successful development of good electrochemical immunoassay, the labeling of biomolecules is usually inevitable because of the limitation of the weakly detectable signal for the antigen-antibody direct reactions.[8] Enzyme labels and nanolabels are usually used for the amplification of electrochemical signal.[9-13] The power and scope of such nanomaterials can be greatly enhanced by coupling with immunoreactions and electrical processes (i.e., nanobioelectronics). Recently, our group successfully synthesized carbon nanotube-based symbiotic coaxial nanocables with nanosilica and gold nanoparticles for the labeling of enzyme-antibody conjugates.[14] Unfortunately, introduction of silica nanostructures into the nanolabels largely decreased the conductivity, thus were not conducive for electron communication during the electrochemical measurement. To improve this issue, mesoporous nanomaterials including magnetic mesoporous $NiCo_2O_4$ nanostructures[15] and mesoporous carbon[16] were also utilized as the labeling of the enzyme-antibody conjugates by using *in situ* synthesis of gold nanostructures in the pore or on the surface. Among these methods, gold nanoparticles were applied for the conjugation with the biomolecules.[17-19] Unfavorably, the growth and assembly of gold nanoparticles were based on the nanostructures with weak conductivity as the seeds. In this regard, the redox reaction and catalytic efficiency of the labeled enzyme on the nanostructures were adequately fulfilled difficultly. An alternative strategy is to utilize the redox-active nanostructures for the assembly of gold nanoparticles.

Prussian blue (iron hexacyanoferrate) is a known, non-toxic blue pigment as well as a widely investigated functional material for the sensors and electrochromics because of the peculiar characteristic of the reduced form of Prussian blue, Prussian White, to catalyze the reduction of H_2O_2 at a low applied potential, thus minimizing the effects of the most common electrochemical interfering species on background currents and signal to noise ratio.[20-22] Prussian blue nanoparticles were easily

synthesized by the addition of aqueous solution of iron (III) ions into an aqueous ferrocyanide solution under vigorous stirring at room temperature.[23] Significantly, Prussian blue nanoparticle could be also used as an electron mediator for rapid electron transfer.[24] In this work, our motivation is to synthesize a new class of redox-active nanostructures including nanogold and Prussian blue nanoparticles for the development of advanced electrochemical immunoassays.

Herein, we devise a new electrochemical immunoassay with signal amplification for quantitative detection of human TPA, as a model analyte, in biological fluids by using Prussian blue-nanogold hybrid microsphere (AuPB) as the label on anti-TPA-functionalized glassy carbon electrode. The as-synthesized AuPB is first used for the labeling of horseradish peroxidase-anti-TPA conjugates through the interaction between gold nanoparticles and proteins. Upon the addition of target TPA, the sandwiched immunocomplex is formed on the as-prepared immunosensor. The carried horseradish peroxidase can catalyze the reduction of hydrogen oxide with the aid of Prussian blue nanoparticles. By monitoring the shift in the cathodic current, we can quantitatively determine the concentration of target TPA in the sample.

Experimental

Reagent and chemicals

Human TPA ELISA kits were purchased from Bioss Biotechnol. Co., Ltd (Beijing, China). The ELISA kits consisted of a series of various-concentration TPA standards and a stock solution of horseradish peroxidase-labeled anti-TPA antibody (HRP-anti-TPA). Horseradish peroxidase (HRP, 250 U mg^{-1}), $HAuCl_4 \cdot 4H_2O$, and bovine serum albumin (BSA, 96–99%) were obtained from Sinopharm Chem. Re. Co., Ltd (Shanghai, China). *N*-Hydroxysuccinimide (NHS) and *N*-(3-dimethylaminopropyl)-*N*′-ethylcarbodiimide hydrochloride (EDC) were obtained from Sigma-Aldrich (Shanghai, China). Aerosol OT (AOT) was the products of Tiantai Fine Chemical (Tianjing, China). All other reagents were of analytical grade and were used without further purification. Ultrapure water obtained from a Millipore water purification system (≥ 18 MΩ, Milli-Q, Millipore) was used in all runs. Phosphate-buffered saline (PBS, 0.1 M) solutions with various pH values were prepared by mixture of the stock solutions of 0.1 M Na_2HPO_4 and 0.1 M NaH_2PO_4, and 0.1 M KCl was used as the supporting electrolyte.

Synthesis of Prussian blue (PB) nanoparticles

Prussian blue (PB) nanoparticles were synthesized consulting to the literatures with a little modification.[25,26] $FeCl_3$ aqueous solution (20 mL, 1.0 mM) containing citric acid (0.8 mmol) was initially added slowly into $K_4[Fe(CN)_6]$ solution (20 mL, 1.0 mM) containing the same-mass citric acid under stirring at 60 ºC. During this process, PB nanoparticles were formed. Following that, the mixture was cooled to room temperature (RT, 22 ± 1.0 ºC), which was centrifuged for 20 min at 11,000 g. Finally, the obtained precipitation (*i.e.* PB nanoparticles) was re-dispersed in distilled water at a concentration of ~30 mg mL^{-1}. The resulting suspension was stored at 4 ºC for further use.

Preparation of nanogold-Prussian blue microspheres (AuPB)

The nanogold-Prussian blue microspheres (designated as AuPB) were prepared by using the reverse micelle method similar to the previous report with some modification.[27] Initially, 0.5 mL of PB suspension (30 mg mL^{-1}) was dropped slowly into 20 mL of 0.1 M AOT iso-octane under vigorous stirring in order to make PB nanoparticles homogeneously disperse in the reverse micellar solution. Following that, 200 µL of 10 wt % $HAuCl_4$ was added slowly in the resulting solution under stirring. Afterward, 100 µL of 0.1 M hydrazine hydrate was injected into the suspension. During this process, Au(III) ions coated on the surface of PB nanoparticles were reduced to zero-valent Au^0 by the hydrazine hydrate. Subsequently, 10 mL of absolute ethanol was added and stirred for 10 min, which resulted in the complete breakdown of reverse micelles with the formation of two immiscible layers of aqueous ethanol and iso-octane because of phase separation. The ethanol was carefully removed using a separating funnel. The particles thus obtained were washed 4 times with iso-octane and centrifuged to remove any residual AOT. The pellets were then dispersed in 10 mL water by vigorous stirring for 30 min and the dispersed system was dialysed against distilled water for 2 h using a 12 kDa cut-off dialysis bag. During this process, the as-synthesized AuPB was present in the bag. Finally, the as-prepared AuPB was dispersed into 1.0-mL distilled water.

Labeling of AuPB with HRP and HRP-anti-TPA

Prior to experiment, the above-prepared AuPB suspension was adjusted to pH 9.0-9.5 by directly using 0.1 M Na_2CO_3 aqueous solution. To achieve a high electrocatalytic signal, AuPB heavily functionalized with HRP and HRP-anti-TPA as follows. Initially, 50 µL of HRP-anti-TPA conjugate (0.2 mg mL^{-1}) and 200 µL of HRP solution (250 U mL^{-1}) were simultaneously added into the above-prepared AuPB colloids. After gently shaking for 5 min, the mixture was transferred to the refrigerator at 4 °C for further reaction (overnight). During this process, HRP and HRP-anti-TPA were conjugated on the surface of AuPB by the dative binding between gold nanoparticles and free -SH groups of the antibody.[28] Following that, the mixture was centrifuged (8,000 g) for 15 min at 4 ºC. The pellet (*i.e.* HRP/HRP-anti-TPA-functionalized AuPB, designated as Bio-AuPB) was re-suspended in 1.0 mL of 2 mM sodium carbonate solution containing 1.0 wt % BSA and 0.1% sodium azide, pH 7.4, and stored at 4 °C until use.

Preparation of electrochemical immunosensor

A glassy carbon electrode (GCE, 3 mm in diameter) was polished repeatedly with 0.3 µm and 0.05 µm alumina slurry, followed by successive sonication in acetone, ethanol and deionized water for 5 min and dried in air. After washing, the cleaned GCE was oxidized at +1.5 V for 15 s in an aqueous solution containing 2.5% $K_2Cr_2O_7$ and 10% HNO_3.[29] During this process, the anodization of the GCE surface resulted in the formation of oxide film with –OH or –COOH. Following that, 6 µL of 5 wt % BSA was thrown on the treated GCE, and dried for 2 h at 60 ºC. The resulting GCE was immersed in pH 7.4 PBS containing 5 mM EDC and 8 mM NHS, and incubated for 4 h at RT. Afterwards, 8 µL of the optimal anti-TPA (0.2 mg mL^{-1}) was dropped on the activated GCE, and reacted for 8 h at 37 ºC. Finally, the anti-TPA-modified GCE was suspended over pH 7.4 PBS at 4 ºC for further use.

Immunoassay protocol and electrochemical measurement

Scheme 1 represents the immunoassay protocol and measurement process of the as-prepared immunosensor toward target TPA. All electrochemical measurements were carried out on a μAutoLab Type III system (Eco Chemie, The Netherlands) with a three-electrode system by using a modified GCE as working electrode, a platinum wire as auxiliary electrode, and an Ag/AgCl as reference electrode. The assay was carried out as follows: (i) 6 μL of TPA standards or samples with various concentrations was thrown on the immunosensor, and incubated for 18 min at RT to form the antigen-antibody complex; (ii) 10 μL (excess) of the above-prepared bio-AuPB suspension was cast on the resulting immunosensor, and incubated for another 18 min to form the sandwiched immunocomplex; and (iii) the resulting immunosensor was monitored in pH 6.8 PBS containing 0.1 mM H_2O_2 by using differential pulse voltammetry (DPV) from 500 to -100 mV (*vs* Ag/AgCl) with a pulse amplitude of 50 mV and a pulse width of 50 ms. The DPV peak current was collected and registered as the sensor signals. After each step, the resulting immunosensor was washed by using pH 7.4 PBS. All measurements were carried out at RT (22 ± 1.0 ºC). Analyses are always made in triplicate.

Results and discussion

Characterization of the as-synthesized AuPB and Bio-AuPB

Typically, gold nanoparticles can be used for the conjugation of proteins through the interaction between cysteine or NH_3^+-lysine residues of proteins and gold nanoparticles. Similar works have been reported for the labeling of biomolecules.[30,31] Use of Prussian blue nanoparticles in this work is expected as the electron mediators to accelerate the electron communication between the labeled HRP and the base electrode. Meanwhile, the doped Prussian blue nanoparticles amongst the microspheres can be also used as the electron donors and acceptors, thus resulting in the amplification of detectable signal. Fig. 1a shows typical transmission electron microscope (TEM) of the as-synthesized AuPB, and the average size was ~50 nm. Moreover, the as-prepared AuPB by using the reverse micelle method could be homogeneously dispersed in the distilled water. Significantly, we also observed that the AuPB consisted of many nanoparticles. Such an open structure could provide a big room for conjugation of the biomolecules. Furthermore, the nanocomposites were also characterized by using energy-dispersive X-ray spectroscope (EDX). As seen from Fig. 1b, Au and Fe elements were obviously appeared in the nanocomposites. The other elements (*e.g.* C, H and O) might be derived from the synthesized agents. The results indicated that AuPB could be successfully prepared by the designed route.

Fig. 1c represents the fourier transform infrared (FTIR) spectra of the synthesized Bio-AuPB. As is well known, the shapes of the infrared absorption bands of amide I groups at 1610-1690 cm^{-1} corresponding to the C=O stretching vibration of peptide linkages and amide II groups around 1500-1600 cm^{-1} from a combination of N-H bending and C-N stretching can provide detailed information on the secondary structure of proteins.[32] Experimental result indicated that two absorption peaks at 1660 and 1560 cm^{-1} could be also observed after the formation of Bio-AuPB, which corresponded to the amide I and II groups of the proteins. The weak band occurred in the region of 1100 cm^{-2} was assigned to the wagging and twisting vibrations of the -CH_2- group in the proteins and were commonly referred to as the progression bands.[33] Therefore, the as-prepared AuPB could be used for the labeling of HRP and HRP-anti-TPA.

Electrochemical characteristics of variously modified electrodes

Fig. 2A shows the cyclic voltammograms of variously modified electrodes at 50 mV s^{-1}. No redox peak was observed at the newly prepared immunosensor in pH 6.8 PBS (curve '*a*'). Such a very low background signal could provide a precondition for highly sensitive detection of target TPA. When the immunosensor reacted with target TPA (10 ng mL^{-1} used in this case), the background current (curve '*b*') decreased relative to that of curve '*a*' in pH 6.8 PBS. The reason might be the fact that the formed immunocomplex had weak conductivity and hindered the electron transfer. After the resulting immunosensor was incubated with the Bio-AuPB, inspiringly, a pair of well-defined redox peaks was achieved in pH 6.8 PBS (curve '*c*'). The result suggested that the doped Prussian blue nanoparticle in the AuPB could maintain its natural redox characteristic.[34] To further monitor the bioactivity of the immobilized HRP on the AuPB, 0.1 mM H_2O_2 as the enzyme substrate was added into pH 6.8 PBS. As shown from curve '*d*', an obvious catalytic characteristic was achieved with an increase of the cathodic current and a decrease of the anodic current. The result indicated that the immobilized HRP onto the AuPB could retain high enzymatic catalytic activity and effectively shuttle electrons from the base electrode surface to the redox center of the HRP.

Logically, a puzzled question to be produced is whether the electrochemical signal derived from the non-specific absorption of the as-prepared immunosensor toward the Bio-AuPB during the incubation process. To clarify this point, the newly prepared immunosensors with the same batch were used for the detection of 0 and 10 ng mL^{-1} TPA (as an example), respectively. Curve '*a*' in Fig. 2B represents the DPV curve of the newly prepared immunosensor. When the immunosensor was incubated with 0 ng mL^{-1} TPA and excess Bio-AuPB in sequence, the DPV peak current (curve '*b*') was almost the same as that of the newly prepared immunosensor (curve '*a*'). In contrast, when the immunosensor was incubated with 10 ng mL^{-1} TPA, the DPV peak current largely increased. These results further revealed that the change in the DPV peak current mainly derived from the specific antigen-antibody reaction between target TPA and anti-TPA antibody. Furthermore, the as-synthesized AuPB could be utilized for the amplification of detectable electrochemical signal.

Optimization of experimental conditions

To achieve an optimal analytical performance, some experimental conditions including the incubation time and incubation temperature for the antigen-antibody reaction, and the conjugated ratio of HRP/HRP-anti-TPA on the AuPB should be optimized (1.0 ng mL^{-1} TPA used in this case). Considering the convenience of the electrochemical immunoassay for future application, we selected at RT (22 ± 1.0 °C) for the antigen-antibody interaction throughout the experiment. At this condition, we monitored the effect of incubation time on the current of the electrochemical immunoassay from 10 min to 35 min (*Note*: To avoid confusion, the incubation times of the immunosensor with TPA were

paralleled with those of the immunosensor-TPA with Bio-AuPB). As seen from Fig. 3a, the electrochemical signal increased with the increasing incubation time, and tended to level off after 18 min. Hence, an incubation time of 18 min was chosen for the detection of TPA at acceptable throughput.

Because of the co-immobilization of HRP and HRP-anti-TPA on the AuPB, the conjugated ratio of HRP and HRP-anti-TPA is one of the most important factors influencing the sensitivity of the electrochemical immunoassay. Usually, the highly carried amount of anti-TPA antibody on the AuPB can increase the possibility of the antigen-antibody reaction, but it is not conducive to the electrochemical measurement because the detectable signal mainly derived from the labeled HRP toward the catalytic reduction of H_2O_2. As shown in Fig. 3b, the maximum signal was obtained at the volume ratio of 4 : 1. So, 200 μL of HRP ($C_{[HRP]}$ = 150 U mL^{-1}) and 50 μL of HRP-anti-TPA (0.2 mg mL^{-1}) was used for the preparation of the Bio-AuPB.

An important parameter is the pH of the assay solution because the catalytic efficiency of bioactive enzyme is usually relative to the pH of the assay solution. Fig. 3c shows the effect of various pH values of PBS on the current responses of the immunoassay in the presence of 0.1 mM H_2O_2 towards 1.0 ng mL^{-1} TPA. As shown in Fig. 3c, the current increased with the increment of pH value from pH 5 to 6.8 and then decreased. The optimal electrochemical signal was achieved at pH 6.8. Highly acidic or alkaline surroundings would damage the immobilized protein, especially in alkalinity. So pH 6.8 of PBS was selected as the electrolyte for the detection of target TPA.

Dose response of the immunoassay toward target TPA

To increase the probability for effective treatment, highly sensitive detection of cancer markers is very important for early cancer diagnosis. Under optimal conditions, the sensitivity and dynamic range of the electrochemical immunoassay were evaluated toward TPA standards in pH 6.8 PBS containing 0.1 mM H_2O_2 by using the Bio-AuPB as the nanotags on anti-TPA-modified GCE with a sandwich-type immunoassay format. As shown from Fig. 4a, the DPV peak currents increased with the increasing of target TPA concentration in the sample. A linear dependence between the peak current and the concentration of target TPA was obtained in the range from 0.01 ng mL^{-1} to 30 ng mL^{-1} with a detection limit (LOD) of 5.0 pg mL^{-1} estimated at the $3S_{blank}$ level (n = 13) (Fig. 4b). The linear regression equation was adjusted to i_{pc} (uA) = -0.7065 $C_{[TPA]}$ – 0.4365 (ng mL^{-1}) (R^2 = 9948, n = 24). Although our designed system has not yet been optimized for maximum efficiency, the LOD of the method was comparable with commercialized MyBioSource Human TPA ELISA Kit (0.05 ng mL^{-1}, Cat# MBS161723), Uscn Human TPA ELISA Kit (28 pg mL^{-1}, Cat# SEA163Hu), BlueGene Human TPA ELISA Kit (1 pg mL^{-1}, Cat# E01T0013), BT Human TPA ELISA Kit (0.05 ng mL^{-1}, Cat# E1655Hu), and USBiological Human TPA ELISA Kit (28 pg mL^{-1}, Cat# 028458).

Precision, reproducibility, specificity and stability

The precision of the electrochemical immunoassay were studied by repeatedly assaying 3 different TPA standards, using identical batches of the Bio-AuPB. Experimental results indicated that the coefficients of variation (CVs) of the intraassay were 8.1, 5.7, and 7.9% (n = 3) for 0.05, 1, and 25 ng mL^{-1} TPA, respectively, whereas the CVs of the inter-assay with various batches were 10.6, 9.3, and 9.6% towards the above-mentioned analytes, respectively. With the exception of the slightly increased CV for the 0.05 ng mL^{-1} standard in the inter-assay experiment, the other CVs suggested that the electrochemical immunoassay could be used repeatedly, and further verified the possibility of the batch preparation. When the as-prepared Bio-AuPB was not in use, they were stored at 4 °C. 95.2%, 90.7%, and 80.3% of the initial signal were preserved at 11th, 19th, and 38th day between the same batches.

The specificity of the electrochemical immunoassay was also evaluated relative to other cancer markers or proteins, *e.g.* alpha-fetoprotein (AFP), prostate-specific antigen (PSA), carcinoma antigen 125 (CA 125) and cancer antigen 19-9 (CA 19-9). The evaluation was carried out with the same assay protocol. As shown from Fig. 5a, when using these interfering agents as the incubation solution alone (20 ng mL^{-1} or 20 U mL^{-1} used in this case), the obtained electrochemical signals were almost the same as the background signal. Significantly, when target TPA (0.1 ng mL^{-1}) and the interfering agents (20 ng mL^{-1} or 20 U mL^{-1}) simultaneously coexisted in the incubation solution, no obvious signals were changed relative to target TPA alone. These results indicated that the compounds coexisting in the sample matrix did not interfere with the detection of target TPA, *i.e.* the designed electrochemical immunoassay revealed sufficiently selective for the monitoring of target TPA.

Analysis of real samples and method validation

To monitor the feasibility and application of the newly developed immunosensing method for the analysis of real samples, we collected 8 clinical human serum specimens from the local hospital and prepared 8 spiked new-born cattle serum samples by using TPA standards. These samples were initially assayed by using the electrochemical immunoassay, and the results were compared with the referenced values obtained from human TPA ELISA kit. Comparison of the experimental results obtained with the electrochemical immunoassay with those of ELISA was implemented by using a least-squares regression method (Fig. 5b). The regression equation was fitted to y = (0.9928 ± 0.13) x – (0.1114 ± 0.2) (R^2 = 0.997, n = 48) where x stands for TPA concentrations estimated with the electrochemical immunoassay and y stands for those of the referenced method. The standard deviations of the slope and intercept are given on the regression equation. The correlation between two methods was investigated using t-tests for comparison of the experimental values of the intercept and slope to the ideal situation of zero intercept and slope of 1. The statistics t for the slope and intercept were calculated respectively as follows: t = (b-1)/s_b and t = (a-0)/s_a where b and a stands for the slope and intercept, respectively, and s_b and s_a for the standard deviation of the slope and intercept, respectively. No significance differences at the 0.05 significance level were encountered between the optimum values of intercept and slope and experimental data, thereby revealing a good agreement between both analytical methods.

Inserting Graphics

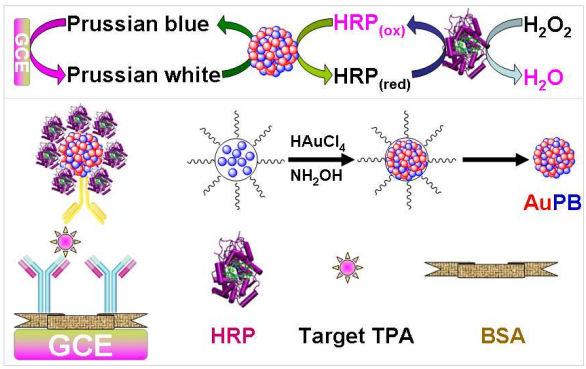

Scheme 1 Schematic illustration of the sandwich-type electrochemical immunoassay using Prussian blue nanoparticles-doped nanogold microspheres as the labels (bottom), and the electron transfer pathway during the electrochemical measurement (top).

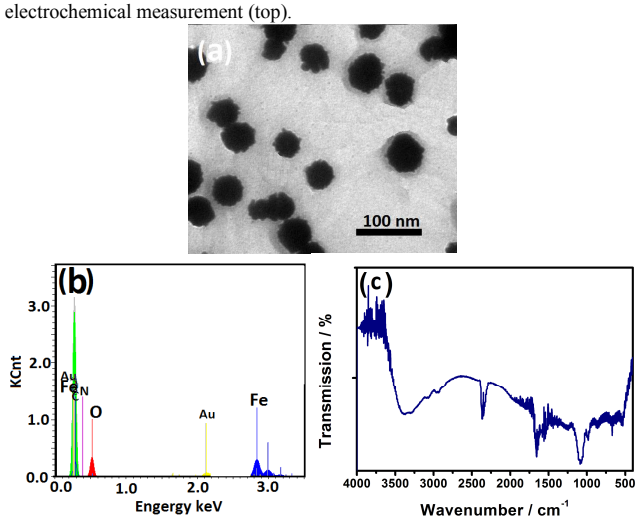

Fig. 1 (a) TEM image and (b) EDX of the as-synthesized AuPB, and (c) FT-IR spectrum of the as-prepared Bio-AuPB.

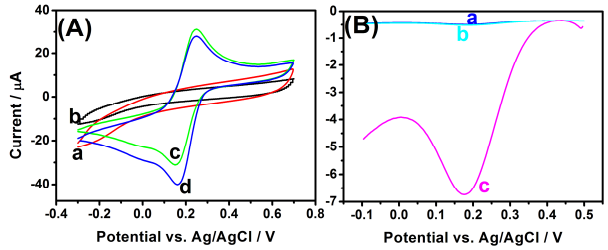

Fig. 2 (A) Cyclic voltammograms of (a) anti-TPA-modified GCE in pH 6.8 PBS, (b) electrode '*a*' after incubation with 10 ng mL^{-1} TPA in pH 6.8 PBS, (c) electrode '*b*' after incubation with excess Bio-AuPB in pH 6.8 PBS, and (d) electrode '*c*' in pH 6.8 PBS containing 0.1 mM H_2O_2 at 50 mV s^{-1}. (B) DPV curves of (a) the newly prepared immunosensor, and (b,c) sensor '*a*' after incubation with (b) 0 + Bio-AuPB and (c) 10 ng mL^{-1} TPA + Bio-AuPB, respectively, in pH 6.8 PBS containing 0.1 mM H_2O_2.

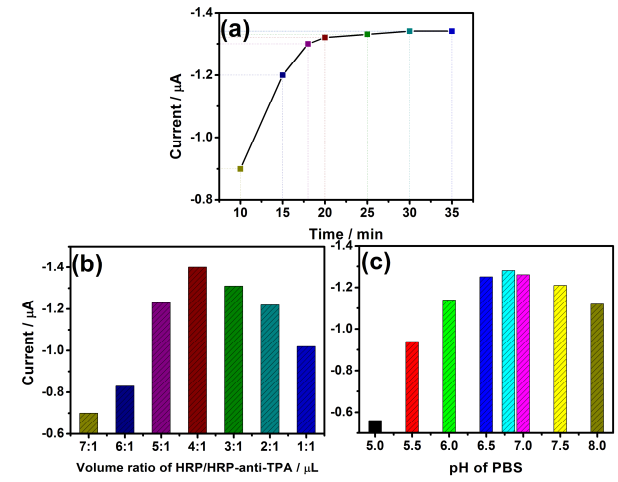

Fig. 3 Effects of (a) incubation time for the antigen-antibody reaction, (b) volume ratio between HRP (150 U mL^{-1}) and HRP-anti-TPA (0.2 mg mL^{-1}) for the preparation of Bio-AuPB, and (c) pH of PBS on the current of the electrochemical immunoassay (1.0 ng mL^{-1} TPA used in this case).

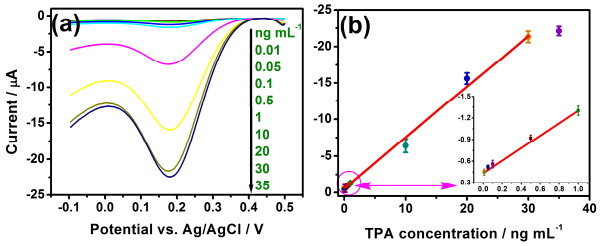

Fig. 4 (a) DPV responses of the electrochemical immunoassay toward target TPA standards in pH 6.8 PBS containing 0.1 mM H_2O_2, and (b) calibration plots (*Inset*: linear curve at the low concentrations range from 0.01 ng mL^{-1} to 1.0 ng mL^{-1}).

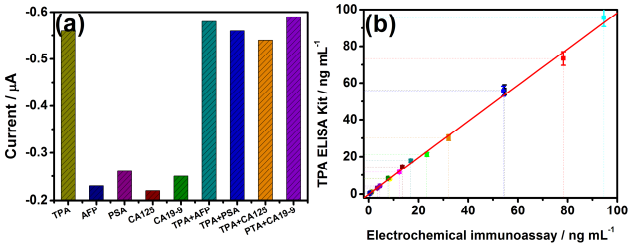

Fig. 5 (a) Selectivity of the electrochemical immunoassay against CA 125, CA 19-9, AFP and PSA, and (b) comparison of the assayed results for 8 clinical serum specimens and 8 spiked new-born cattle serum samples using the electrochemical immunoassay and the referenced human TPA ELISA Kit (*Note*: The high-concentration TPA samples were calculated according to the dilution ratio).

Conclusions

In summary, this work reports on the proof-of-concept of a new signal-amplification strategy for the development of advanced sandwich-type electrochemical immunoassay by using the redox-active Prussian blue-nanogold microspheres as the labeling of signal antibody. In comparsion with nanogold or nanogold-functionalized semiconducting labels, the as-synthesized AuPB exhibits high conductivity, and facilitates the electron transfer.

Importantly, introduction of Prussian blue nanoparticles amongst the nanolabels can avoid the addition of external mediators in the detection solution, thus reducing the contamination. Highlight of this work is to efficiently utilize good-conductivity Prussian blue and high-compatibility gold nanoparticles for the labelling of signal tags. Preferably, the detectable signal of the developed immunoassay can be amplified by tuning the conjugation ratio with the bioactive enzyme and secondary antibody. Importantly, the methodology opens a new horizen for the design of high-conducting nanolabels. Future work should be focused on other low-abundance proteins by controlling the target antibody, thus representing the versatility of the assay scheme.

This project was funded by the International Collaboration Program of Guizhou Province, China (Grant 2011-7016; to Q.L.). This work was also supported in part by the Grant 41176079 from the National Natural Science Foundation of China and the Grant 2010CB732403 from the "973" National Basic Research Program of China (to D. T.).

Notes and references

[a] *College of Pharmaceutical Sciences, Zunyi Medical University, Zunyi 563003, P.R. China; Fax:+86 852 8609343; Tel: +86 852 8609337; E-mail: slinder809@126.com (Q. Li);* [b] *Key Laboratory of Analysis and Detection for Food Safety (Ministry of Education & Fujian Province), Department of Chemistry, Fuzhou University, 350108 Fuzhou, P.R. China. Fax: +86 591 2286 6135; Tel: +86 591 2286 6125; E-mail: dianping.tang@fzu.edu.cn (D. Tang)*

1 Y. Zheng, Y. Chen, M. Hu, Y. Lin and Y. Chen, *Chin. German J. Clin. Oncology*, 2012, **11**, 655-659.
2 S. Xie, X. Ding, W. Mo and J. Chen, Acta Histochem., 2013, doi: j.actthis.2013.09.001.
3 H. van Poppel, J. Billen, H. Goethuys, A. Elgamal, M. Gerits, L. Mortelmans, N. Blanckaert and L. Baert, *Anticancer Res*., 1996, **16**, 2205-2207.
4 Z. Yao, K. Huang, J. Guo, Y. Li, J. Yu and F. Wu, *J. Nanosci. Nanotechnol*., 2012, **12**, 112-118.
5 D. Tang, B. Su, J. Tang, J. Ren and G. Chen, *Anal. Chem*., 2010, **82**, 1527-1534.
6 B. Zhang, B. Liu, J. Liao, G. Chen and D. Tang, *Anal. Chem.*, 2013, **85**, 9245-9252.
7 C. Woolley and M. Hayes, *Bioanalysis*, 2013, **5**, 245-264.
8 J. Rushling, *Anal. Chem*., 2013, **85**, 5304-5310.
9 K. Omidfar, F. Khorsand and M. Darziani Azizi, *Biosens. Bioelectron.*, 2013, **43**, 336-347.
10 M. Hasanzadeh, N. Shadjou, E. Omidinia, M. Eskandani and M. de la Guardia, *TrAC-Anal. Chem*., 2013, **45**, 93-106.
11 X. Pei, B. Zhang, J. Tang, B. Liu, W. Lai and D. Tang. *Anal. Chim. Acta*, 2013, **758**, 1-18.
12 W. Wei, M. Wei and S. Liu, *Rev. Anal. Chem*., 2012, **31**, 163-176.
13 D. Tang, Y. Cui and G. Chen, *Analyst*, 2013, **138**, 981-990.
14 Q. Li, D. Tang, J. Tang, B. Su, J. Huang and G. Chen, *Talanta*, 2011, **84**, 538-546.
15 Q. Li, L. Zeng, J. Wang, D. Tang, D. Tang, B. Liu, G. Chen and M. Wei, *ACS Appl. Mater. Interfaces*, 2011, **3**, 1366-1373.
16 L. Zeng, Q. Li, D. Tang, G. Chen and M. Wei, *Electrochim. Acta*, 2012, **68**, 158-165.
17 B. Chikkaveeraiah, A. Bhirde, N. Morgan, H. Eden and X. Chen, *ACS Nano*, 2012, **6**, 6546-6561.
18 S. Gopinath, T. Lakshmipriya and K. Awazu, *Biosens. Bioelectron*., 2014, **51**, 115-123.
19 J. Zhang, B. Liu, H. Liu, X. Zhang and W. Tan, *Nanomedicine*, 2013, **8**, 983-993.
20 M. Magro, D. Baratella, G. Salviulo, K. Polakova, G. Zoppellaro, J. Tucek, J. Kaslik, R. Zboril and F. Vianello, *Biosens. Bioelectron*., 2014, **52**, 159-165.
21 D. Feng, X. Lu, X. Dong, Y. Ling and Y. Zhang, *Microchim. Acta*, 2013, **180**, 767-774.
22 S. Pintado, S. Goberna-Ferron, E. Escudero-Adan and J. Galan-Mascaros, *J. Am. Chem. Soc*., 2013, **135**, 13270-13273.
23 A. Farah, N. Shooto, F. Thema, J. Modise and E. Diko, *Int. J. Electrochem. Sci*., 2012, **7**, 4302-4313.
24 Z. Chu, L. Shi, Y. Liu, W. Jin and N. Xu, *Biosens. Bioelectron*., 2013, **47**, 329-334.
25 X. Liang, Z. Deng, L. Jing, X. Li, Z. Dai, C. Li and M. Huang, *Chem. Commun*., 203, **49**, 11029-11031.
26 S. Wang, C. Chen and L. Chen, *Sci. Technol. Adv. Mater.*, 2013, **14**, 044405.
27 D. Tang and J. Ren, *Anal. Chem*., 2008, **80**, 8064-8070.
28 Z. Gao, M. Xu, L. Hou, G. Chen and D. Tang, *Anal. Chem*., 2013, **85**, 6945-6952.
29 J. Tang, J. Zhou, Q. Li, D. Tang, G. Chen and H. Yang, *Chem. Commun*., 2013, **49**, 1530-1532.
30 C. Yu, L. Huang, D. Kwan, W. Wakarchuk, S. Withers and C. Lin, *Chem. Commun*., 2013, **49**, 10166-10168.
31 H. Hinterwirth, G. Stubiger, W. Lindner and M. Lammerhofer, *Anal. Chem.*, 2013, **85**, 8376-8384.
32 M. Jackson, L. Choo and P. Watson, *Biochem. Biophys. Acta*, 1995, **1270**, 1-6.
33 S. Dong, G. Luo, J. Feng, Q. Li and H. Gao, *Electroanalysis*, 2001, **13**, 30-33.
34 G. Wang, G. Zhang, H. Huang and L. Wang, *Anal. Methods*, 2011, **3**, 2082-2087.